PROCEEDINGS OF SCIENCE

Study of R_{AA} and v_2 of non-strange D mesons and D-jet production in Pb–Pb collisions with ALICE

Fabrizio Grosa* **on behalf of the ALICE Collaboration**
Politecnico di Torino, Corso Duca degli Abruzzi 24, 10129 Torino Italy
INFN sez. Torino, via Pietro Giuria 1, 10125 Torino Italy
E-mail: fabrizio.grosa@cern.ch

Heavy quarks are sensitive probes of the colour-deconfined medium formed in ultra-relativistic heavy-ion collisions, the Quark–Gluon Plasma (QGP). The ALICE Collaboration measured the production of D^0, D^+, and D^{*+} mesons in Pb–Pb collisions at $\sqrt{s_{NN}} = 5.02$ TeV. The properties of the in-medium energy loss are investigated via the measurement of the nuclear modification factor (R_{AA}) of non-strange D mesons. The modification of the D-meson transverse momentum (p_T) distributions inside the jet is studied via the measurement of the D-meson tagged jet R_{AA} in central Pb–Pb collisions. In mid-central collisions, the measurement of the D-meson elliptic flow (v_2) at low and intermediate p_T gives insight into the participation of the charm quark in the collective motion of the system, while at high p_T it constrains the path-length dependence of the energy loss. The coupling of the charm quark to the light quarks in the underlying medium is further investigated with the application of the event-shape engineering (ESE) technique to D-meson elliptic flow.

PoS(EPS-HEP2019)280

European Physical Society Conference on High Energy Physics - EPS-HEP2019 -
10-17 July, 2019
Ghent, Belgium

*Speaker.

1. Introduction

In ultra-relativistic heavy-ion collisions, heavy quarks (charm and beauty) are produced in the early times of the reaction via hard-scattering processes and they subsequently probe the colour-deconfined medium, known as Quark–Gluon Plasma (QGP). The measurement of the nuclear modification factor ($R_{\rm AA}$) of hadrons containing heavy quarks, defined as the ratio between the $p_{\rm T}$-differential yields in nucleus–nucleus collisions ($\mathrm{d}N_{\rm AA}/\mathrm{d}p_{\rm T}$) and the $p_{\rm T}$-differential production cross section measured in pp collisions ($\mathrm{d}\sigma_{\rm pp}/\mathrm{d}p_{\rm T}$) scaled by the average nuclear overlap function $\langle T_{\rm AA}\rangle$, is used to study the properties of the in-medium parton energy loss. The comparison to light-flavour hadrons provides information about the quark-mass and colour-charge dependence, while the measurement of the charm jets can be used to study the modification of the internal jet sub-structure in the medium.

Further insights into the interaction of heavy quarks with the QGP are given by the measurement of azimuthal anisotropies, which are typically characterised in terms of Fourier coefficients, $v_{\rm n} = \langle \cos {\rm n}(\varphi - \Psi_{\rm n})\rangle$, where φ is the particle-momentum azimuthal angle, the brackets denote the average over all the measured particles in the considered events, and $\Psi_{\rm n}$ is the symmetry-plane angle relative to the nth harmonic. The second-harmonic coefficient, called elliptic flow, is the dominant term in mid-central heavy-ion collisions due to the almond-shaped interaction region. At low $p_{\rm T}$ it is sensitive to the participation in the collective dynamics of the underlying medium and the degree of thermalisation of the heavy quarks in the medium, while at high $p_{\rm T}$ it is governed by the path-length dependence of the parton energy loss in the medium.

2. D-meson and jet reconstruction

Open-charm production in Pb–Pb collisions at $\sqrt{s_{\rm NN}} = 5.02$ TeV was measured by ALICE via the exclusive reconstruction of D mesons at mid-rapidity ($|y| < 0.8$), in the hadronic decay channels $\mathrm{D}^0 \to \mathrm{K}^-\pi^+$ ($c\tau \simeq 123$ μm, BR = 3.89%), $\mathrm{D}^+ \to \mathrm{K}^-\pi^+\pi^+$ ($c\tau \simeq 312$ μm, BR = 8.98%), and $\mathrm{D}^{*+} \to \mathrm{D}^0\pi^+ \to \mathrm{K}^-\pi^+\pi^+$ (strong decay, BR = 2.63%) [1]. The decay topologies were reconstructed exploiting the excellent vertex-reconstruction capabilities of the Inner Tracking System (ITS). Kaons and pions were identified with the Time Projection Chamber (TPC) via their specific energy loss and with the Time-Of-Flight detector (TOF). The raw D-meson yields were extracted via an invariant-mass analysis after having applied topological selections to enhance the signal over background ratio. The efficiency-times-acceptance corrections were obtained from MC simulations based on HIJING [2] and PYTHIA6 [3] event generators and the GEANT3 transport package [4]. The fraction of prompt D mesons was estimated with a FONLL-based approach [5, 6]. The centrality and the direction of the event plane (estimator of Ψ_2) were provided by the V0 scintillators, which cover the pseudorapidity regions $-3.7 < \eta < -1.7$ (V0C) and $2.8 < \eta < 5.1$ (V0A). The measurement of the D-meson v_2 was performed with the scalar-product (SP) method [7]. The D^0-meson tagged charged jets were reconstructed with the FASTJET package [8] and the anti-$k_{\rm T}$ clustering algorithm [9] using charged-particle tracks and requiring the presence of the daughter tracks of a D^0 meson among the jet constituents. The covered charged-jet transverse-momentum range was $5 < p_{\rm T,\,ch\,jet} < 20$ GeV/c, with the jet resolution parameter $R = 0.3$ and a requirement of the D-meson transverse momentum $p_{\rm T,D} > 3$ GeV/c. The background density scaled by the area of the

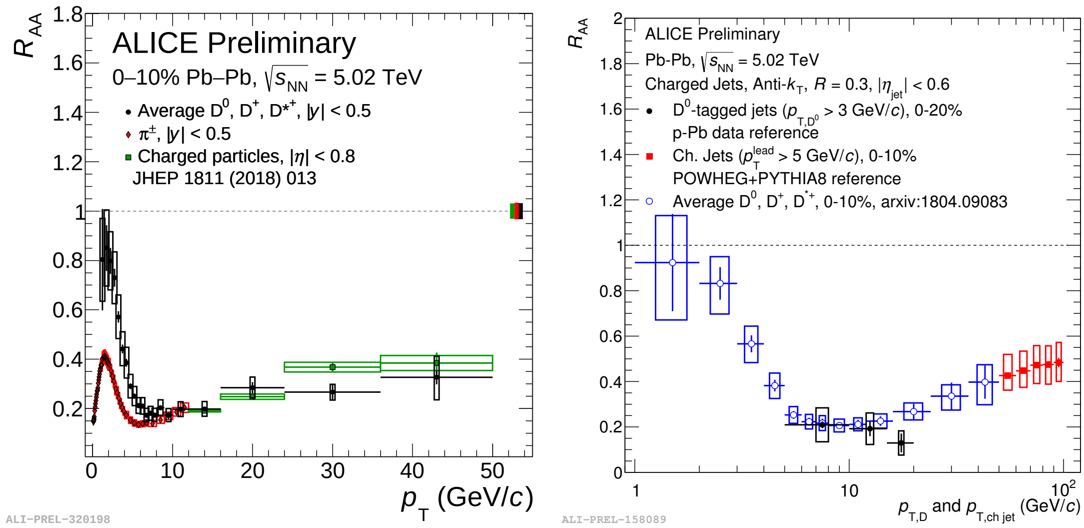

Figure 1: Average prompt D^0, D^+, and D^{*+} R_{AA} in Pb–Pb collisions at $\sqrt{s_{NN}} = 5.02$ TeV in the 0–10% centrality class compared to the R_{AA} of $\pi^{\pm}$ for $p_T < 12$ GeV$/c$ and charged particle R_{AA} for $p_T > 12$ GeV$/c$ (left panel) and to the R_{AA} of charged jets and D^0-meson tagged jets in the 0–20% centrality class (right panel).

reconstructed signal jet was subtracted from the reconstructed p_T of the signal jet. The underlying background momentum density was estimated event-by-event using the median of $p^{raw,k_T}_{T,\,ch\,jet}/A_{jet}$, where $p^{raw,k_T}_{T,\,ch\,jet}$ is the uncorrected $p_{T,\,ch\,jet}$ and A_{jet} is the area of the jets reconstructed with the k_T algorithm. The $p^{raw}_{T,\,ch\,jet}$ spectrum of the jets reconstructed with the anti-k_T algorithm was then unfolded for the detector response and the background fluctuations in the underlying event extracted using the random cone method [10].

3. D-meson nuclear modification factor

The left panel of Fig. 1 shows the average R_{AA} of prompt D^0, D^+, and D^{*+} mesons measured in the 10% most central Pb–Pb collisions at $\sqrt{s_{NN}} = 5.02$ TeV. It is compared to the charged-pion and charged-particle [11] R_{AA} measured at the same energy and centrality class for $p_T < 12$ GeV$/c$ and $p_T > 12$ GeV$/c$, respectively. The R_{AA} of D mesons is higher than that of charged pions by more than $2\,\sigma$ in each p_T bin for $p_T < 6$ GeV$/c$, suggesting a quark-mass dependence of the in-medium energy loss. This observation is however nontrivial, since several other effects can contribute to this difference, such as the different scaling of soft and hard probes at low p_T, the different initial shapes of p_T spectra, different contributions of radial flow and hadronisation via recombination.

In the right panel of Fig. 1, the R_{AA} of D^0-tagged jets is shown. A strong suppression, similar to that of the prompt D-meson [12] is observed.

Figure 2 shows the comparison between the measured D-meson R_{AA} and that predicted by theoretical models based on perturbative QCD (pQCD) calculations of high p_T charm-quark energy loss [13, 14, 15] (left panel) and charm-quark transport in a hydrodynamically expanding medium [16, 17, 18, 19, 20, 21] (right panel). The R_{AA} for $p_T > 10$ GeV$/c$ is well described by pQCD-based models, as well as by the MC@sHQ+EPOS2 and LIDO models. The low p_T re-

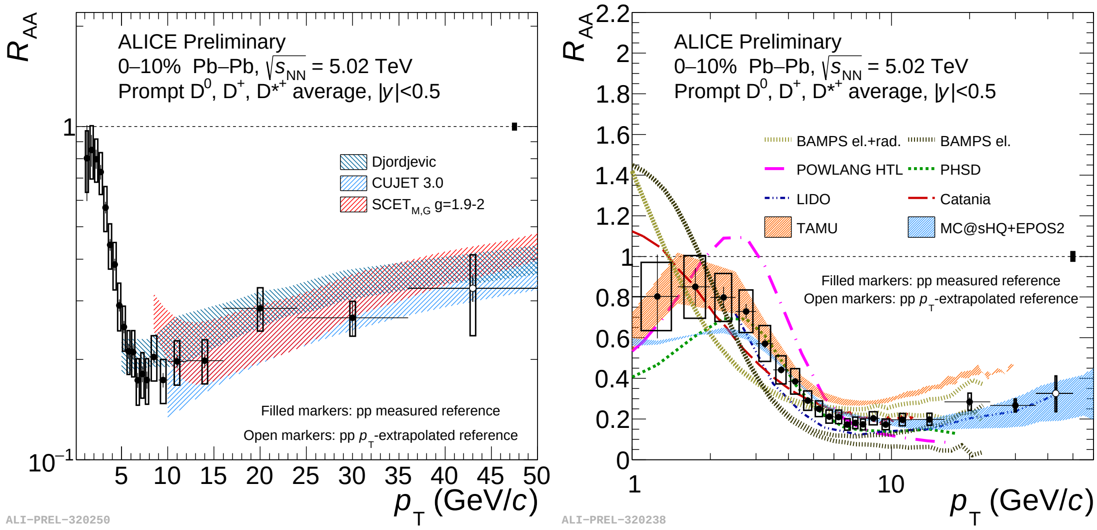

Figure 2: Average prompt D^0, D$^+$, and D^{*+} R_{AA} in Pb–Pb collisions at $\sqrt{s_{NN}} = 5.02$ TeV in the 0–10% centrality class compared to model predictions based on pQCD calculations of parton energy loss (left panel) and on the charm-quark transport in an expanding medium (right panel).

gion of the measured R_{AA} is fairly reproduced by most of the models that implement charm-quark transport.

4. D-meson azimuthal anisotropies

Figure 3 shows the average v_2 of prompt D^0, D$^+$, and D^{*+} measured in mid-central (30–50%) Pb–Pb collisions at $\sqrt{s_{NN}} = 5.02$ TeV, compared to that of charged pions [22] for $p_T < 15$ GeV/c, charged particles [23] for $p_T > 15$ GeV/c at mid-rapidity, and inclusive J/ψ mesons at forward rapidity [24].

The average prompt D-meson v_2 was found to be lower (similar) to that of charged pions for $p_T < 3$ GeV/c ($p_T > 3$ GeV/c) and higher than that of J/ψ mesons for $p_T < 6$ GeV/c. This observation is consistent with the scaling of the v_2 with the mass of the meson species observed for light-flavour hadrons below 3 GeV/c [22], and the increase of the D-meson v_2 due to the hadronisation of the charm quark via recombination with flowing light-flavour quarks [25]. The measured v_2 coefficients for all the meson species converge to a similar value for $p_T > 6-8$ GeV/c, as expected when the path-length dependence of the in-medium parton energy loss is the mechanisms that originates the azimuthal anisotropy.

The v_2 of D^0, D$^+$, and D^{*+} mesons was further investigated applying the event-shape engineering (ESE) technique [7]. This technique relies on the classification of events with fixed centrality but different average elliptic flow, quantified by the magnitude of the second-harmonic reduced flow vector, $q_2^{TPC} = |\boldsymbol{Q}_2^{TPC}|/\sqrt{M}$, where M is the multiplicity and $\boldsymbol{Q}_2^{TPC}$ is the second-harmonic flow vector measured with charged-particle tracks reconstructed in the TPC detector having $|\eta| < 0.8$ [26].

The D-meson v_2 was found to be higher (lower) in the 20% of events with largest (smallest) q_2^{TPC}, confirming a correlation between the D-meson azimuthal anisotropy and the collective expansion of the bulk matter.

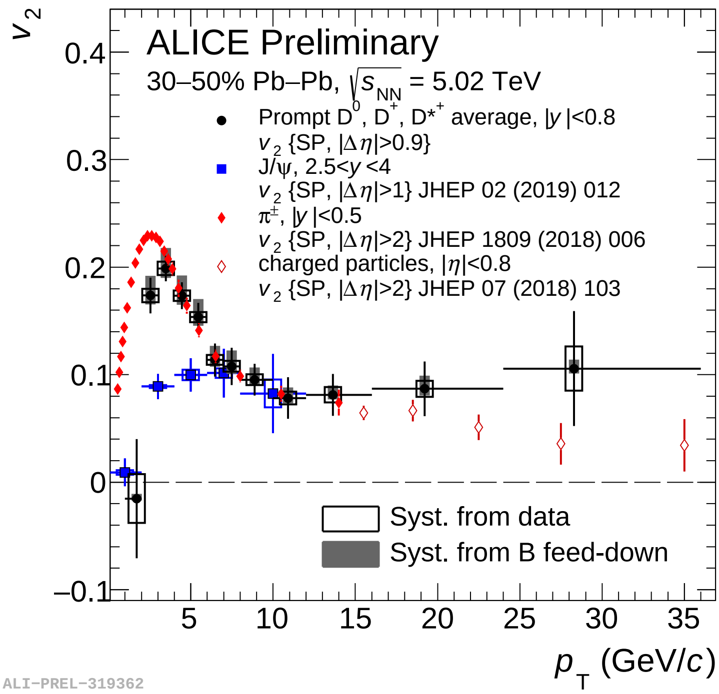

Figure 3: Average prompt D^0, D$^+$, and D^{*+} v_2 in Pb–Pb collisions at $\sqrt{s_{NN}} = 5.02$ TeV in the 30–50% centrality class, compared to that of charged pions [22] for $p_T < 15$ GeV$/c$, charged particles [23] for $p_T > 15$ GeV$/c$ at mid-rapidity, and inclusive J$/\psi$ mesons at forward rapidity [24].

The top panels of Fig. 4 show the average v_2 of prompt D mesons measured in the samples of events with 20% smallest q_2^{TPC}, 20% largest q_2^{TPC}, and without ESE selection (unbiased sample) compared to the predictions provided by models that implement the charm-quark transport in a hydrodynamically expanding medium. In the bottom panels of the same figure, the ratios of the v_2 in the ESE-selected and unbiased samples are displayed. The POWLANG [27] model describes the measurements in the unbiased and 20% large-q_2^{TPC} samples, while it underestimates the measurement in the small-q_2^{TPC} sample. Conversely, the DAB-MOD [28] and LIDO [18] models better describe the measured D-meson v_2 in the small-q_2^{TPC} sample and underestimate those in the unbiased and large-q_2^{TPC} samples.

5. Conclusions

In this contribution, the most recent results on the production and azimuthal anisotropy of D mesons, measured in Pb–Pb collisions at $\sqrt{s_{NN}} = 5.02$ TeV, were presented. The measurements of the D-meson R_{AA} and v_2, performed on the latest sample of Pb–Pb collisions collected in 2018, have an improved statistical precision by about a factor three (two) in the 0–10% (30–50%) centrality class compared to the previous results published by the ALICE Collaboration [6, 12, 26]. The first measurement of the D^0-meson tagged jet R_{AA} in Pb–Pb collisions, performed with the data sample collected in 2015, was also presented. The precision of the measurement and the $p_{T,\,ch\,jet}$ reach will be greatly improved with the sample of Pb–Pb collisions collected in 2018.

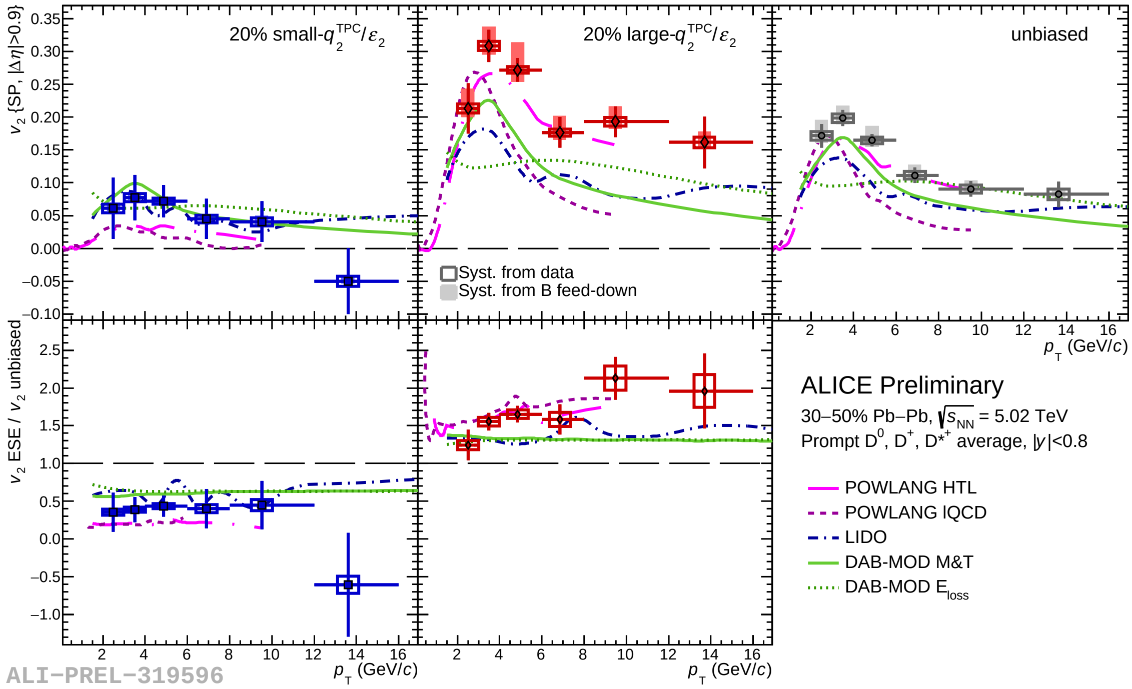

Figure 4: Average prompt D^0, D$^+$, and D^{*+} v_2 in Pb–Pb collisions at $\sqrt{s_{NN}} = 5.02$ TeV in the 30–50% centrality class, for the small-q_2^{TPC} (top-left panel), large-q_2^{TPC} (top-middle panel), and unbiased (top-right panel) samples compared to transport models. The ratios between the v_2 in the ESE-selected and unbiased samples are displayed in the bottom panels.

References

[1] **PDG** Collaboration, "*Review of Particle Physics*," *Phys. Rev.* **D98** no.~3, (2018) 030001.

[2] X.-N. Wang and M. Gyulassy, "*HIJING: A Monte Carlo model for multiple jet production in p p, p A and A A collisions*," *Phys. Rev.* **D44** (1991) 3501–3516.

[3] T. Sjostrand, S. Mrenna, and P. Z. Skands, "*PYTHIA 6.4 Physics and Manual*," *JHEP* **05** (2006) 026, arXiv:hep-ph/0603175.

[4] R. Brun, F. Bruyant, F. Carminati, S. Giani, M. Maire, A. McPherson, G. Patrick, and L. Urban, "*GEANT Detector Description and Simulation Tool*,".

[5] M. Cacciari, M. Greco, and P. Nason, "*The P(T) spectrum in heavy flavor hadroproduction*," *JHEP* **05** (1998) 007, arXiv:hep-ph/9803400.

[6] **ALICE** Collaboration, "*D-meson azimuthal anisotropy in midcentral Pb-Pb collisions at* $\sqrt{s_{NN}} = \mathbf{5.02}$ *TeV*," *Phys. Rev. Lett.* **120** no.~10, (2018) 102301, arXiv:1707.01005.

[7] S. A. Voloshin, A. M. Poskanzer, and R. Snellings, "*Collective phenomena in non-central nuclear collisions*," *Landolt-Bornstein* **23** (2010) 293–333, arXiv:0809.2949.

[8] M. Cacciari, G. P. Salam, and G. Soyez, "*FastJet User Manual*," *Eur. Phys. J.* **C72** (2012) 1896, arXiv:1111.6097.

[9] M. Cacciari, G. P. Salam, and G. Soyez, "*The anti-k_t jet clustering algorithm*," *JHEP* **04** (2008) 063, arXiv:0802.1189.

[10] **ALICE** Collaboration, "*Measurement of Event Background Fluctuations for Charged Particle Jet Reconstruction in Pb-Pb collisions at $\sqrt{s_{NN}} = 2.76$ TeV*," *JHEP* **03** (2012) 053, arXiv:1201.2423.

[11] **ALICE** Collaboration, "*Transverse momentum spectra and nuclear modification factors of charged particles in pp, p-Pb and Pb-Pb collisions at the LHC*," *JHEP* **11** (2018) 013, arXiv:1802.09145.

[12] **ALICE** Collaboration, "*Measurement of D^0, D^+, D^{*+} and D_s^+ production in Pb-Pb collisions at $\sqrt{s_{NN}} = 5.02$ TeV*," *JHEP* **10** (2018) 174, arXiv:1804.09083.

[13] M. Djordjevic, "*Heavy flavor puzzle at LHC: a serendipitous interplay of jet suppression and fragmentation*," *Phys. Rev. Lett.* **112** no.~4, (2014) 042302, arXiv:1307.4702.

[14] J. Xu, J. Liao, and M. Gyulassy, "*Bridging Soft-Hard Transport Properties of Quark-Gluon Plasmas with CUJET3.0*," *JHEP* **02** (2016) 169, arXiv:1508.00552.

[15] Z.-B. Kang, F. Ringer, and I. Vitev, "*Effective field theory approach to open heavy flavor production in heavy-ion collisions*," *JHEP* **03** (2017) 146, arXiv:1610.02043.

[16] J. Aichelin, P. B. Gossiaux, and T. Gousset, "*Radiative and Collisional Energy Loss of Heavy Quarks in Deconfined Matter*," *Acta Phys. Polon.* **B43** (2012) 655–662, arXiv:1201.4192.

[17] T. Song, H. Berrehrah, D. Cabrera, W. Cassing, and E. Bratkovskaya, "*Charm production in Pb + Pb collisions at energies available at the CERN Large Hadron Collider*," *Phys. Rev.* **C93** no.~3, (2016) 034906, arXiv:1512.00891.

[18] W. Ke, Y. Xu, and S. A. Bass, "*Linearized Boltzmann-Langevin model for heavy quark transport in hot and dense QCD matter*," *Phys. Rev.* **C98** no.~6, (2018) 064901, arXiv:1806.08848.

[19] J. Uphoff, O. Fochler, Z. Xu, and C. Greiner, "*Elastic and radiative heavy quark interactions in ultra-relativistic heavy-ion collisions*," *J. Phys.* **G42** no.~11, (2015) 115106, arXiv:1408.2964.

[20] M. He, R. J. Fries, and R. Rapp, "*Heavy Flavor at the Large Hadron Collider in a Strong Coupling Approach*," *Phys. Lett.* **B735** (2014) 445–450, arXiv:1401.3817.

[21] A. Beraudo, A. De Pace, M. Monteno, M. Nardi, and F. Prino, "*Heavy flavors in heavy-ion collisions: quenching, flow and correlations*," *Eur. Phys. J.* **C75** no.~3, (2015) 121, arXiv:1410.6082.

[22] **ALICE** Collaboration, "*Anisotropic flow of identified particles in Pb-Pb collisions at $\sqrt{s}_{NN} = 5.02$ TeV*," *JHEP* **09** (2018) 006, arXiv:1805.04390.

[23] **ALICE** Collaboration, "*Energy dependence and fluctuations of anisotropic flow in Pb-Pb collisions at $\sqrt{s_{NN}} = 5.02$ and 2.76 TeV*," *JHEP* **07** (2018) 103, arXiv:1804.02944.

[24] **ALICE** Collaboration, "*Study of J/ψ azimuthal anisotropy at forward rapidity in Pb-Pb collisions at $\sqrt{s_{NN}} = 5.02$ TeV*," *JHEP* **02** (2019) 012, arXiv:1811.12727.

[25] M. Nahrgang, J. Aichelin, S. Bass, P. B. Gossiaux, and K. Werner, "*Elliptic and triangular flow of heavy flavor in heavy-ion collisions*," *Phys. Rev.* **C91** no.~1, (2015) 014904, arXiv:1410.5396.

[26] **ALICE** Collaboration, "*Event-shape engineering for the D-meson elliptic flow in mid-central Pb-Pb collisions at $\sqrt{s_{NN}} = 5.02$ TeV*," *JHEP* **02** (2019) 150, arXiv:1809.09371.

[27] A. Beraudo, A. De Pace, M. Monteno, M. Nardi, and F. Prino, "*Event-shape engineering and heavy-flavour observables in relativistic heavy-ion collisions*," *Eur. Phys. J.* **C79** no.~6, (2019) 494, arXiv:1812.08337.

[28] R. Katz, C. A. G. Prado, J. Noronha-Hostler, J. Noronha, and A. A. P. Suaide, "*DAB-MOD sensitivity study of heavy flavor R_{AA} and azimuthal anisotropies based on beam energy, initial conditions, hadronization, and suppression mechanisms*," arXiv:1906.10768.